

1 **Supplementary Materials**

2 **The PDF file includes:**

3 Supplementary Notes 1-3

4 Figs. S1 to S5

5 Tables S1 to S4

6

7

8

9

10

11

12

13

14

15

16

17

18

19

20

21

22

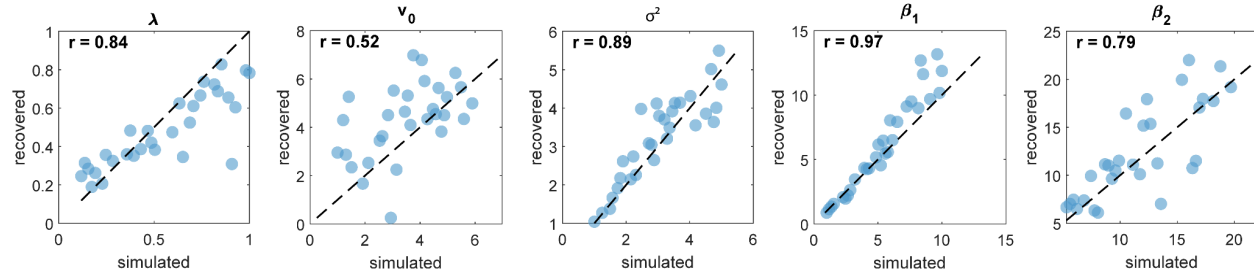
23

24 **Supplementary Notes1. Parameter recovery**

25 We conducted a comprehensive parameter recovery analysis to validate our model
26 fitting procedure. We generated synthetic data from 30 artificial subjects using the
27 binary VKF combined with a softmax choice model. For parameter estimation, we
28 employed the same Hierarchical Bayesian Inference (HBI) approach used in our
29 empirical data analysis. To ensure robust estimation and minimize random variation
30 effects, we repeated this procedure 20 times with different random seeds.

31 The recovery analysis revealed strong correlations between the true and recovered
32 parameters, with median correlation coefficients across the 20 simulations: $r_\lambda = 0.852$,
33 $r_{v_0} = 0.473$, $r_{\sigma^2} = 0.919$, $r_{\beta_1} = 0.918$, $r_{\beta_2} = 0.782$.

34 For the visualization aim, we plotted relationships between simulated parameters and
35 recovered parameters for one of the simulations (Fig. S1)



37 **Fig. S1. Parameter recovery analysis.**

38 The scatter plots show the relationship between simulated (true) and recovered
39 parameters for the binary VKF model with softmax choice rule. Each point represents
40 one artificial subject (n=30). The dashed lines indicate perfect recovery ($y=x$).
41 Correlation coefficients (r) are shown for each parameter. Parameters shown are step
42 size (λ), initial volatility parameter(v_0), observational noise (ω), and choice sensitivity
43 parameters (β_1 , β_2).

44 Note: Parameters were estimated using Hierarchical Bayesian Inference (HBI).
45 Correlations indicate strong parameter recovery for most parameters, with moderate
46 recovery for initial uncertainty (v_0).

47 Control analyses for initial volatility parameter(v_0)

48 While our main analyses treated the initial volatility parameter (v_0) as a free parameter,
49 we observed a relatively lower recovery rate for v_0 compared to other parameters. Here
50 we demonstrate that this lower recovery rate does not compromise the model's
51 reliability or our main conclusions.

52 First, to validate our parameter estimation's robustness, we systematically analyzed
53 parameter recovery across different fixed values ($\underline{\nu}_0=[1, 3, 5, 7, 9]$). Using the same set
54 of simulated data, we found that the recovery rates for the key parameters (λ , σ^2 , β_1 ,
55 β_2) remained stable regardless of the fixed $\underline{\nu}_0$ value. Specifically, the correlations
56 between true and recovered parameters maintained consistent levels ($r_\lambda = 0.852$, $r_{\sigma^2} =$
57 0.949 , $r_{\beta_1} = 0.937$, $r_{\beta_2} = 0.831$) across all $\underline{\nu}_0$ values, suggesting that $\underline{\nu}_0$ does not
58 substantially interact with the recovery of other parameters.

59 Furthermore, when we compared model fits with $\underline{\nu}_0$ fixed at 5, the VKF-RVRU model still
60 outperformed alternative models ($BIC_{RW1}=13343$, $BIC_{RW2}=13303$, $BIC_{KF}=13481$,
61 $BIC_{VKF}=13467$, $BIC_{VKF-RU}=13996$, $BIC_{VKF-RVRU}=\mathbf{13243}$), consistent with our main
62 findings using the full model with free $\underline{\nu}_0$. This invariance to $\underline{\nu}_0$ demonstrates that while
63 $\underline{\nu}_0$ shows lower recovery rates, this does not affect the model's ability to capture the key
64 learning dynamics or our ability to reliably estimate the central parameters governing
65 these dynamics. These results support our decision to retain $\underline{\nu}_0$ as a free parameter in
66 the main analyses while providing evidence that its lower recovery rate does not impact
67 the robustness of our primary findings.

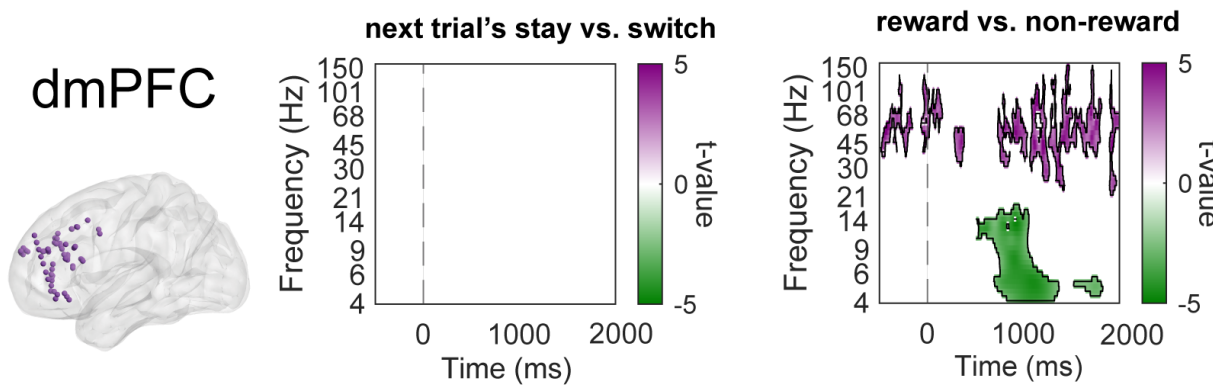
68

69

70 **Supplementary Notes 2. dmPFC did not signal subsequent decisions in feedback**
71 **stage**

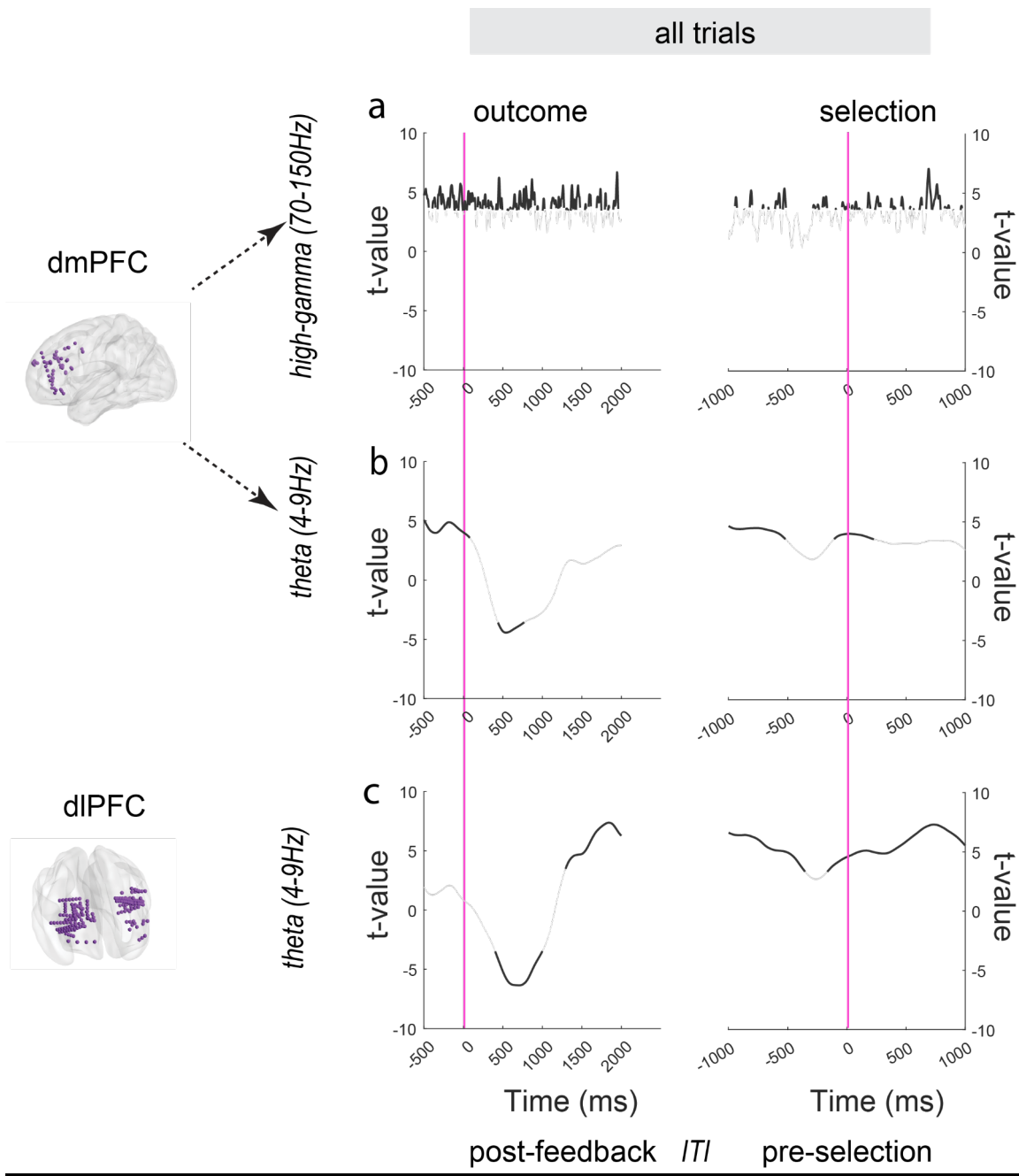
72
73 We already know (from [Fig. 2](#)), that the dmPFC did not differentiate between stay versus
74 switch in the pre-selection stage. To further investigate whether dmPFC participates in
75 action selection in the feedback stage, we analyzed its neural activity during the
76 feedback stage using a linear mixed-effects model:

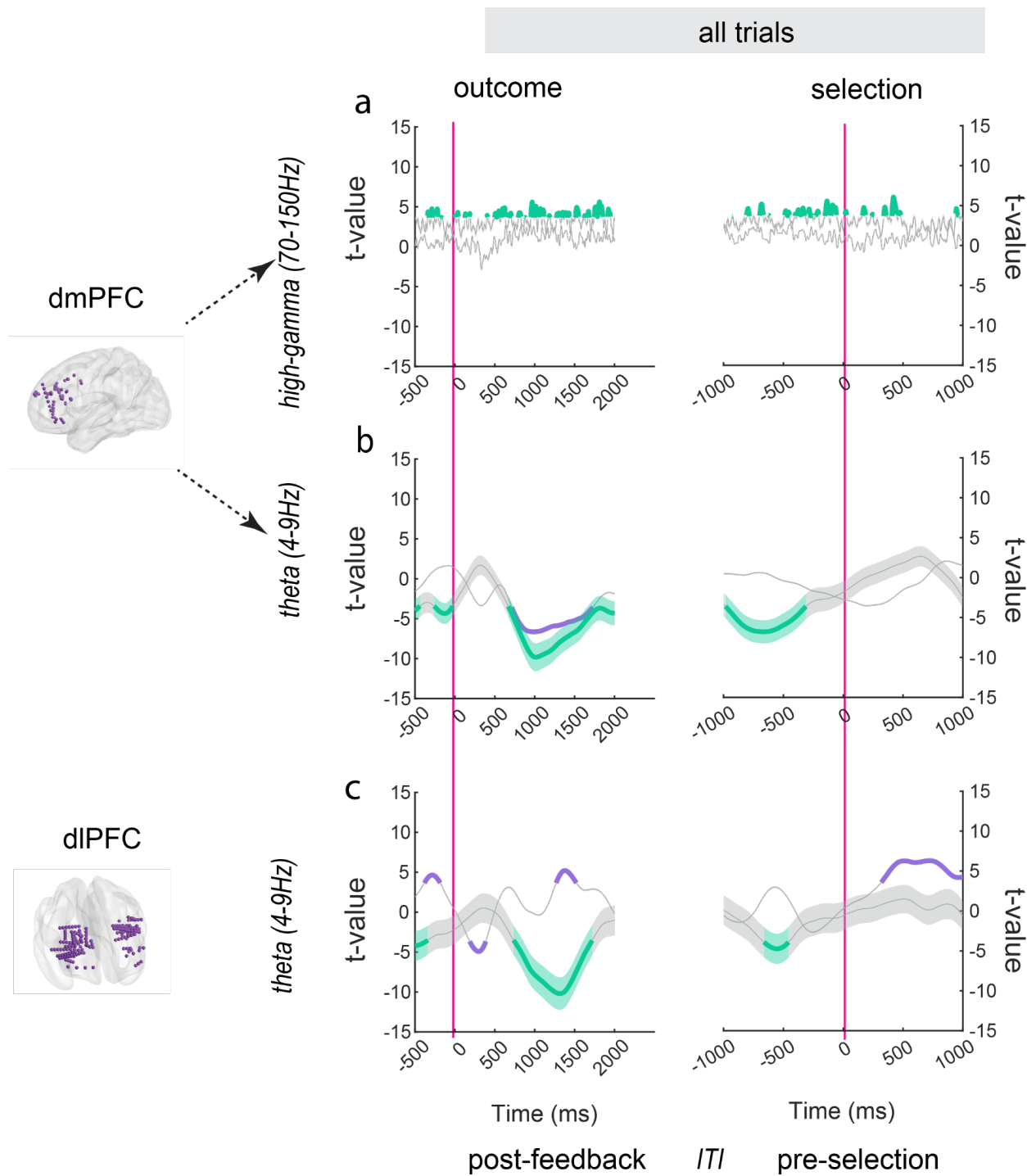
77
78 $erd \sim \underline{\text{NextTrials' (Stay vs. Switch)}} + \text{reward (reward vs. non-reward)} + \text{previous trial}$
79 $\text{feedback} + (1|\text{patientID}) + (1|\text{channelID:patientID})$
80 Time-frequency analyses revealed no significant clusters differentiating between
81 subsequent stay versus switch decisions in the dmPFC ([Fig. S2](#), left panel). However,
82 the dmPFC showed robust outcome-related activity, with distinct spectral signatures for
83 reward versus non-reward feedback in both high-gamma (70-150 Hz) and theta (4-9 Hz)
84 bands ([Fig. S2](#), right panel). These results support our main finding that dmPFC
85 primarily processes feedback information rather than directly encoding subsequent
86 behavioral choices.



88 **Fig. S2. dmPFC activity reflects feedback processing but not subsequent**
89 **decisions**

90 Time-frequency maps showing T-values from linear mixed-effects regression analyses
91 of dmPFC local field potentials during feedback processing. Left: No significant
92 differences between trials preceding stay versus switch decisions. Right: Significant
93 differences between reward and non-reward feedback, particularly in high-gamma and
94 theta bands. Color scales represent T-values, with warmer colors indicating higher
95 values. Black outlines indicate significant clusters (cluster-based permutation tests,
96 5000 permutations, $p < 0.05$). Time 0 represents feedback onset. Frequency bands are
97 displayed on the y-axis, ranging from 4 Hz to 150Hz.



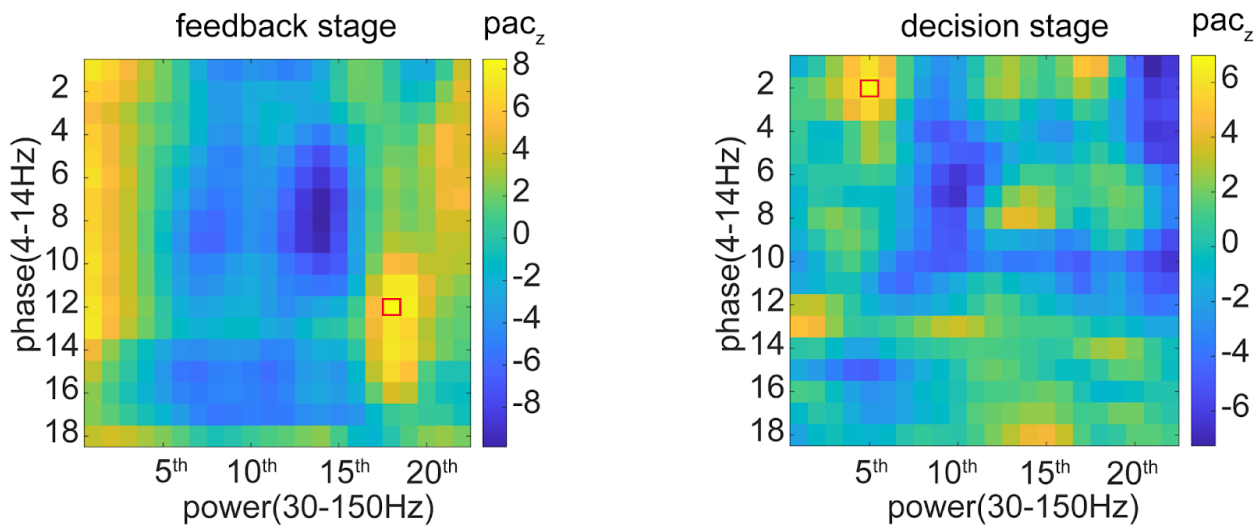


108

109 **Fig. S4. Neural representations of relative value and uncertainty in dlPFC and**
 110 **dmPFC across all trials.**

111 (a) dmPFC high-gamma band (70-150 Hz), (b) dmPFC theta band (4-9 Hz), and (c)
 112 dlPFC theta band showing robust PE representation. Lines represent t-values from
 113 linear mixed-effects regression, with shaded areas indicating SEM. Horizontal bars
 114 beneath each plot indicate periods of significant encoding ($p < 0.05$, cluster-corrected).

115
116
117



118

119

120 **Fig. S5. Phase-amplitude coupling analysis between dmPFC high-frequency
121 power and dIPFC low-frequency phase**

122 Each panel shows a grid map of PAC z-values (permutation, 1000 times) for different
123 frequency combinations. The x-axis shows the indices (5th, 10th, 15th, 20th) from the
124 logarithmically spaced high-frequency power bands (30-150 Hz), while the y-axis shows
125 the indices (2nd, 4th, 6th, ..., 18th) from the logarithmically spaced low-frequency phase
126 bands (4-14 Hz). Each cell in the grid represents the PAC z-value for that specific
127 phase-amplitude frequency combination, averaged across all trials and patients. Color
128 intensity indicates the strength of coupling, with warmer colors representing stronger
129 PAC.

130

131

132

133

134

135

136

Table S1. Patients demographics

ID	Gender	Age	handedness	Completed trial numbers
P01	Male	35	R	509
P02	Male	29	R	274
P03	Female	25	R	161
P04	Male	35	R	699
P05	Female	55	R	524
P06	Male	51	R	914
P07	Male	37	R	864
P08	Female	43	R	689
P09	Male	57	R	300
P10	Male	32	R	764
P11	Male	34	L	758
P12	Male	32	R	192
P13	Female	61	R	90
P14	Male	33	R	453

138 **Notes:** This table summarizes the patient demographics in the study. The table includes
139 information on each patient's ID, gender, age, handedness, and the number of
140 completed trials.

141

142 **Table S2. Behavioral indices and response times**

	Stay %	Switch %	Win. Stay	Lose.shift	RT _{stay}	RT _{switch}	RT _{win-stay}	RT _{lose-switch}
Mean	0.446	0.516	0.599	0.749	1.046	1.06	1.014	1.01
SD	0.183	0.174	0.249	0.148	0.451	0.384	0.424	0.374

143 **Notes:** Model-free behavioral measures and response times (RT) across participants.
144 Stay % = percentage of trials where participants repeated their previous choice;
145 Switch % = percentage of trials where participants changed their choice; Win-Stay =
146 percentage of trials where participants repeated their choice following reward; Lose-
147 Switch = percentage of trials where participants changed their choice following no
148 reward; RT_{stay} = response time for stay decisions (in seconds); RT_{switch} = response time
149 for switch decisions (in seconds); RT_{win-stay} = response time for stay decisions following
150 reward (in seconds); RT_{lose-switch} = response time for switch decisions following no
151 reward (in seconds). Values are shown as mean ± standard deviation across
152 participants.

153 **Table S3. More time information**

	The interval between selection and outcome onset within the same trial	Inter-trial interval
Mean	0.461	0.626
SD	0.216	0.072

154 **Notes:** Values are shown as mean ± standard deviation across participants.

155

156 **Table S4. Model performance**

All models	XP (exceedance probabilities)	BIC
RW1	0.169	13343
RW2	0.006	13303
KF	0.001	13481
VKF	0.001	13544
VKF-RU	0.001	14043
VKF-RVRU	0.822	13294

157 **Notes:** Model comparison results using exceedance probabilities (XP) and Bayesian
158 Information Criterion (BIC). Lower BIC values indicate better model fit. RW1 = standard
159 Rescorla-Wagner model with single learning rate; RW2 = Rescorla-Wagner model with
160 separate learning rates for reward and no-reward; KF = standard Kalman filter; VKF =
161 volatile Kalman filter; VKF-RU = volatile Kalman filter with relative uncertainty; VKF-
162 RVRU = volatile Kalman filter incorporating both relative value and relative uncertainty.
163 The VKF-RVRU model showed the highest XP and lowest BIC, indicating it best
164 explains participants' choice behavior.

165

166